SALAMANDRA **59**(1): 63–77
15 February 2023 | ISSN 0036–3375

SALAMANDRA
German Journal of Herpetology

Disentangling the biogeographic history of a truly pan-Amazonian amphibian – the case of the three-striped poison frog, *Ameerega trivittata* (Dendrobatidae: Colostethinae)

Michael Mayer[1], Philipp Böning[1], Albertina P. Lima[2], Henrik Krehenwinkel[1], Youszef O. C. Bitar[3], Paulo S. Bernarde[4], Michael Veith[1], Moises B. de Souza[5] & Stefan Lötters[1]

[1] Trier University, Department of Biogeography, 54286 Trier, Germany
[2] Instituto Nacional de Pesquisas da Amazônia, Coordenação de Biodiversidade, 69080-971, Manaus, AM, Brazil
[3] Universidade Federal do Pará, Campus Universitário do Marajó-Soure, Laboratório de Ecologia de Comunidades, 68870-000 Soure, PA, Brazil
[4] Universidade Federal do Acre, Campus Floresta, 69980-000, Cruzeiro do Sul, AC, Brazil
[5] Universidade Federal do Acre, Centro de Ciências Biológicas e da Natureza, 69915-900, Rio Branco, AC, Brazil

Corresponding author: Stefan Lötters, ORCID-ID: 0000-0002-7187-1968, e-mail: loetters@uni-trier.de

Manuscript received: 12 December 2022
Accepted: 23 January 2023 by Jörn Köhler

Abstract. Anuran amphibians have intensively been studied to understand Amazonian biodiversity. Improved methods and sampling has revealed that many widespread nominal species in fact are complexes of species with smaller allopatric ranges. Pan-Amazonian anuran species are rather an exception. In a case study using the three-striped poison frog (Anura: Dendrobatidae: *Ameerega trivittata*), we ask how the pan-Amazonian distribution of this taxon can be explained and hypothesize that dispersal has played a major role. Species delimitation and intraspecific relationships of the study species were examined from novel and existing (GenBank) sequences of the mitochondrial 16S rRNA gene from 108 specimens of 38 localities using maximum likelihood and Bayesian methods. We performed BioGeoBEARS models using a time-calibrated population tree to reconstruct the biogeographic history. Our results support that *A. trivittata* is a pan-Amazonian species scattered over its geographic range. Being of Late Miocene origin, the species rapidly spread into newly available space and repeatedly dispersed for-and backward, while vicariance played a major role only in the Early Pliocene. We suggest that intrinsic morphological and life history characteristics (adult size, relative reproductive success) make *A. trivittata* a more successful disperser than other species, so that riverine barriers are more permeable and hamper allopatric speciation. We conclude that there is no universal causality explaining Amazonia biodiversity, because species-specific biological characteristics are key determents of biogeographical histories. Comparatively better dispersal advantages foster larger geographic ranges and can explain pan-Amazonian distributions.

Key words. Amphibia, Anura, BioGeoBEARS, dispersal, genetic diversity, mitochondrial DNA, Neotropics, riverine barrier, vicariance, widespread species.

Introduction

The Amazon basin of South America is one of the regions with the highest biological diversity on earth (Jenkins et al. 2013, Antonelli et al. 2015). There have been various hypotheses about the diversification processes of its extant biota (Hill & Hill 2001, Hoorn et al. 2010, Rull & Carnaval 2020). However, studies on both plants and animals revealed that there is no universal causality to explain species richness in Amazonia. Rather, for particular groups, the biogeographical history is more unique. Reasons include species-specific life history traits, biotic interaction, habitat availability, river course change, geological age and geographic origin (Collevatti et al. 2009, Leite & Rogers 2013, Antonelli et al. 2018, Cracraft et al. 2020,). This is well exemplified in the more than 600 extant amphibian species, most of which belonging to the order Anura (e.g. Mayer et al. 2019). A variety of hypotheses have been invoked to explain the species richness within different taxa (reviewed by Leite & Rogers 2013).

Some examples for anuran taxa are given in the following. Noonan & Gaucher (2005) demonstrated incomplete speciation processes due to repeated secondary contact in harlequin toads of the genus *Atelopus* from the

eastern Guiana Shield in the frame of the Disturbance Vicariance hypothesis. The widely invoked river-barrier hypothesis was demonstrated to be applicable to tree frogs (*Dendropsophus leucophyllatus* complex) by Pirani et al. (2019), suggesting dispersal rather than vicariance scenarios. Réjaud et al. (2020), using poison frogs of the genus *Allobates*, showed that allopatric speciation (i.e. vicariance) played a key role for explaining species richness in the upper Amazon basin, while the lower basin and its vicinities were colonized mainly via dispersal.

So far, there is no hypothesis explaining the evolutionary biogeography of pan-Amazonian anurans. There might be a simple reason for this. While in the past, many Amazonian anurans were thought to encompass large distributions – ranging from the Andean versant in the west upper basin to the Guiana Shield in the north-east (e.g. Lynch 1979) – more recent studies demonstrated that this is not the case. Many of the nominal species with large Amazonian distributions actually represent complexes of allopatric cryptic taxa with much smaller geographic ranges (Fouquet et al. 2007, 2012, 2014, Padial & De la Riva 2009, Angulo & Icochea 2010, Brown et al. 2011, Funk et al. 2012, Gehara et al. 2014, Peloso et al. 2014, Vacher et al. 2017, Rojas et al. 2018). As a result, truly pan-Amazonian anuran species are rather an exception that yet have received little attention.

One pan-Amazonian species is the three-striped poison frog *Ameerega trivittata* (Spix, 1824), a member of the family Dendrobatidae, subfamily Colostethinae (Fig. 1). It is one of the largest (adult snout–vent length 35–55 mm) and most widespread species of the entire superfamily Dendrobatoidea (Grant et al. 2006, Lötters et al. 2007). The conspecificy of morphs allocable to *A. trivittata* from different Amazonian terra firme forest localities has been proposed on the basis of morphology (Silverstone 1976) and molecular genetics (Roberts et al. 2006, Grant et al. 2017, Guillory et al. 2020). According to Santos et al. (2009), *A. trivittata* originated in the Amazon basin in the Late Miocene and Guillory et al. (2020) suggested that this was around 7.57 Mya.

Based on literature information on the geological history of the Amazon basin, we develop some scenarios that may help explaining the evolutionary biogeography of *A. trivittata*. With the emergence of the Amazon run-

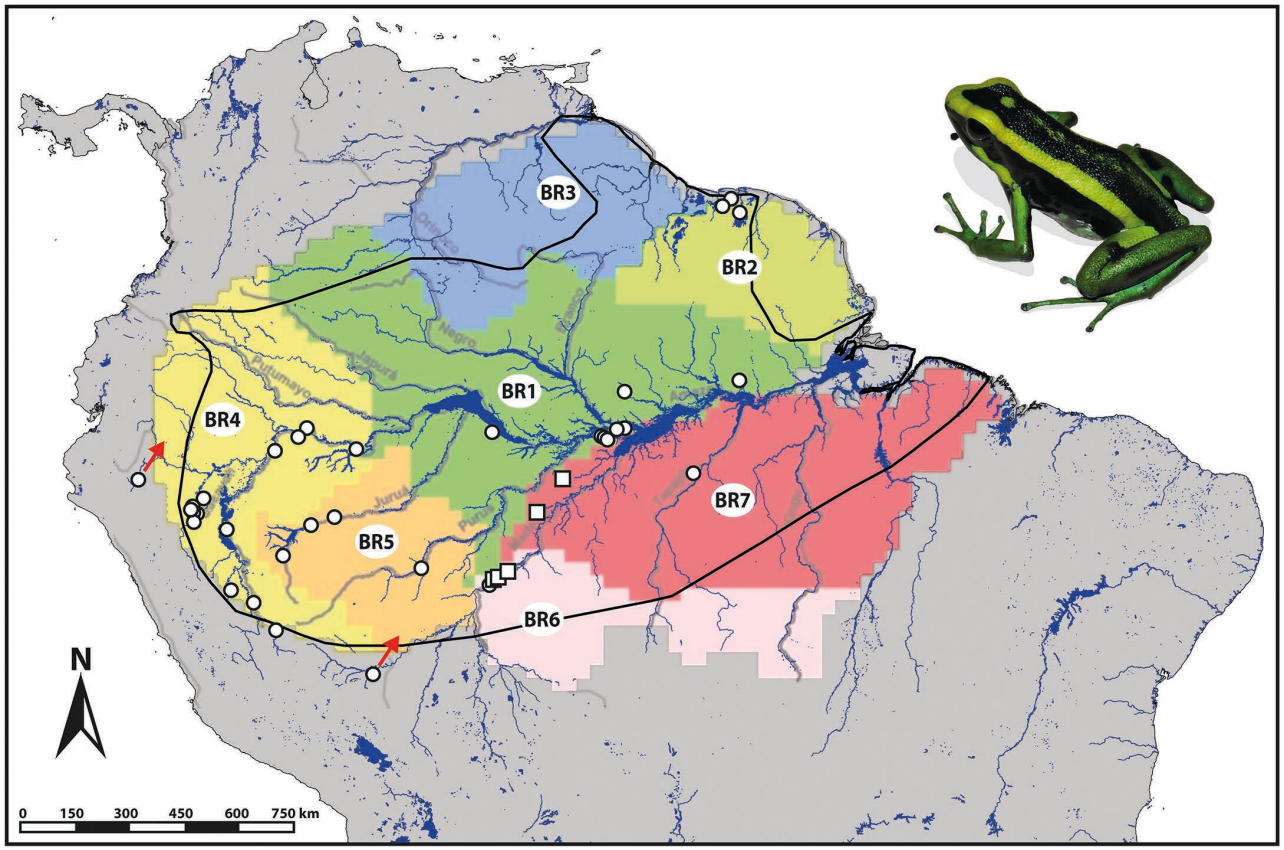

Figure 1. Schematic map of northern South America showing localities of *Ameerega trivittata* investigated in this study (white symbols) and their allocation to biogeographic regions (BR1-BR7 after Godinho & Silva 2018, including colors). Samples of the Madeira River group (see text) are shown as squares, whereas all other samples are given as dots. Two localities outside BRs were provisionally allocated to their nearest BR (indicated by red arrows; Soldado Oliva and Puerto Maldonado, respectively, Table 1). The geographic range of *A. trivittata* as suggested by the IUCN is indicated by a solid line (https://www.iucnredlist.org, accessed 13 February 2022).

ning into the Atlantic Ocean and starting around 8 Mya (Shephard et al. 2010), *A. trivittata* may have expanded its distribution within central Amazonia. Such a scenario is postulated in various taxa (Hoorn et al. 2010) and we assume this for *A. trivittata*, too. Subsequent to that, starting circa 7–6 Mya, enormous water retention bodies formatted in western and central Amazonia, that today are known as major Amazon tributaries (cf. Hoorn et al. 2010, Shephard et al. 2010). It is highly expectable that these water bodies were barriers to *A. trivittata* (as a terra firme species), so that populations became separated. However, when around 5 Mya water bodies opened into the Amazon and became rivers (Hoorn et al. 2010, Albert et al. 2018), they were perhaps permeable to *A. trivittata* allowing multi-directional dispersal and genetic exchange. We base this assumption on the observation that, in anurans, larger body size has been shown to be beneficial for dispersal (Wollenberg et al. 2011, Searcy et al. 2018).

Using a molecular genetic approach (1) we here test for conspecificy of pan-Amazonian *A. trivittata* populations using an enlarged geographic sampling. We expect all samples to belong to a single species based on (A) low genetic diversity and (B) representing a monophyletic assemblage. In line with the one-species-hypothesis, we expect (C) that *A. trivittata* recently invaded into various directions. Examining the phylogenetic architecture in a spatio-temporal context and using biogeographic modelling, (2) we test for and expect early (Late Miocene) vicariance and subsequent (Pliocene to Pleistocene) dispersal events in this species.

Methods

Sampling and data preparation

Ameerega trivittata samples were collected from 2014 to 2016 at different localities in Brazil and Peru (Tab. 1). For these collections with use the following permits: SISBIO45202-1/2, 15PE 000174/SP, (authorized by permits 0196-2014-MINAGRI-DGFFS/DGEFFS, 0050-2015-SERFOR-DDGGSPFFS-DGSPFS, 312-2015-SERFOR-DGGSPFFS-DGSPFS) and completed with samples from scientific collections. Samples were sequenced (see below). Additional sequences were obtained from GenBank (Benson et al. 2015; https://www.ncbi.nlm.nih.gov/genbank/, accessed 18 December 2021). In total, the complete dataset comprised 108 specimens from 38 localities throughout most of the known geographic range of *A. trivittata* (cf. Silverstone 1976, Lötters et al. 2007). See Supplementary Table S1 for sampling locality details and GenBank accession numbers.

Of these, 36 localities fall into six of the seven biogeographic regions (BR) suggested for Amazonian anuran diversity (Godinho & Silva 2018). We provisionally allocated the two remaining localities to the existing BRs in their vicinities (Fig. 1). In the manner of similar studies (e.g. Réjaud et al. 2020), we use these widely acknowledged spatial units for biogeographic modelling (see below).

We conducted direct sequencing with PCR primers on an automated Sanger sequencer to obtain DNA sequences of the mitochondrial 16S rRNA gene fragment. This marker was chosen because it is suggested to adequately reflect genetic variability within and between species (e.g. Vences et al. 2007). In addition, this marker has recently been successfully used to study the biogeography of several Amazonian amphibians (e.g. Réjaud et al. 2020, Fouquet et al. 2021a,b). We analyzed 83 samples of *A. trivittata*. Genomic DNA was isolated using the QIAGEN DNeasy Tissue Kit, following the manufacturer's guidelines. We performed polymerase chain reaction (PCR) with primers of the mitochondrial gene fragment 16S rRNA (16Sal 5'-CGC CTG TTT ATC AAA AAC AT-3' and 16Sbh 5'-CCG GTC TGA ACT CAG ATC ACG T-3') of Palumbi et al. (2002). This fragment was amplified using an initial denaturation step of 2 min at 94°C, followed by 35 cycles of denaturation at 94°C for 30 s, annealing at 54°C for 90 s and extension at 65°C for 90 s. PCR products were purified using spin columns (QIAGEN). Standard Sanger sequencing was performed directly using the corresponding PCR primers and ABI Big Dye on an ABI3730XL sequencer. Each sample was sequenced twice in forward and reverse directions and complementary sequences were aligned (in total 611 bp). Chromatograms were checked and edited visually. Sequences were deposited in GenBank (for accession numbers see Supplementary Table S1).

We used Mega 10.1 (Kumar et al. 2018) for sequence alignment and analysis. We trimmed initial and end portions of the sequences to 484 bp, so no missing data appeared. Sequences were aligned with Muscle with default parameters (Edgar 2004) as implemented in Mega. Haplotypes were identified and analyzed with DnaSP 6.12.03 (Rozas et al. 2017). We created the final haplotype alignment with GBlocks 0.91.1 (Castresana 2000, Talavera & Castresana 2007; https://ngphylogeny.fr, accessed 24 April 2022) using standard settings and allowed gap positions 'with half' (Massana et al. 2004, Manichanh et al. 2008). This collapsed our dataset into 36 haplotypes, in part occurring at multiple sample sites, resulting in 57 sequences which were used for all analyses (Tab. 1).

TPM2uf+I+G was identified as the best-fitting substitution model with JModelTest 2.1.10 (Darriba et al. 2012), based on the corrected Akaike Information Criterion (AICc). When this model was not implemented in the software used, we applied the K80+I+G or the GTR+I+G model (see below).

Species delimitation

Goal (1A) was to test if genetic samples assigned to *A. trivittata* represent the same taxon. For this purpose, we used three approaches: Pairwise distances (i.e. uncorrected p-values), Generalized Mixed Yule Coalescent model (GMYC; Pons et al. 2006, Fujisawa & Barraclough

Table 1. Sampled *Ameerega trivittata* localities classified to biogeographic regions (BR) with identified haplotypes (H1-H36). Localities: * Madeira River group (see text); ** not in BRs, here provisionally allocated to BRs (see Fig. 1).

Biogeographic region	Country	Locality	Longitude	Latitude	Haplotypes (N)
BR1	Brazil	Tefé	-3.46444	-64.67972	H15(3)
	Brazil	Alenquer	-1.45639	-55.09750	H3(5)
	Brazil	Lago Miriti	-3.32161	-59.54158	H2(1), H20(1), H21(1), H26(1)
	Brazil	Manaquiri	-3.68948	-60.33507	H24(3), H25(1)
	Brazil	Manaus 1	-3.35338	-59.85563	H22(1)
	Brazil	Manaus 2	-3.66866	-60.30093	H2(2), H23(1)
	Brazil	Castanho, 40 km S Manaus	-3.61956	-60.45511	H2(3)
	Brazil	Uatumã River, Balbina	-1.91015	-59.54855	H3(1)
BR2	Suriname	Kabo Forestry Concession	5.26642	-55.75567	H3(1)
	Suriname	Paramaribo-Apura road	5.55848	-55.42227	H3(1)
	Suriname	Brokopondo	5.02026	-55.07899	H3(1)
BR4	Peru	Tahuayo	-4.31400	-73.23259	H14(1)
	Peru	Manati River	-3.65201	-72.20045	H13(1)
	Peru	Bolognesi	-10.06923	-73.91740	H27(6), H28(1), H29(1), H30(1)
	Peru	Contamana	-7.22536	-74.95925	H7(2), H12(5), H31(1)
	Peru	Panguana	-9.58333	-74.80000	H4(2), H32(3), H33(2), H34(1), H35(1), H36(1)
	Peru	Sepahua	-11.13100	-73.05800	H7(8), H27(1)
	Peru	Pebas	-3.31285	-71.85243	H6(1)
	Peru	Shucushuyaco	-6.03204	-75.85705	H9(1)
	Peru	Cainarachi Valley	-6.33289	-76.28336	H9(2)
	Peru	Shapaja	-6.58088	-76.26275	H9(1)
	Peru	Chumilla	-6.61859	-76.18432	H11(1)
	Peru	Tarapoto	-6.46161	-76.35080	H9(1), H10(1)
	Peru	Cordillera Azul	-6.93666	-76.23903	H12(1)
	Peru	Soldado Oliva**	-5.30416	-78.38802	H9(1)
	Colombia	Leticia	-4.12330	-69.94910	H6(3)
BR5	Brazil	Purus River, Camicuã	-8.72703	-67.42433	H5(4)
	Brazil	Juruá River, Ipixuna	-7.05225	-71.69469	H17(1)
	Brazil	Juruá River, Seringal do Condor	-6.74825	-70.78964	H18(1)
	Brazil	Porto Walter	-8.24875	-72.78001	H7(8), H8(1)
	Peru	Puerto Maldonado**	-12.83715	-69.29372	H5(2)
BR6	Brazil	Madeira River, Ilha do Búfalo*	-9.14375	-64.51606	H1(3)
	Brazil	Madeira River, Jirau Direito	-9.32417	-64.71083	H5(1)
	Brazil	Madeira River, Ilha da Pedra*	-9.15889	-64.63389	H1(2), H16(1)
	Brazil	Madeira River, Teotônio*	-8.84788	-64.06847	H1(1)
BR7	Brazil	Madeira River, Castanho*	-5.26545	-61.94445	H1(1)
	Brazil	Madeira River, Humaitá*	-6.56312	-62.93648	H19(2)
	Brazil	Tapajós River, left side	-5.06892	-56.87200	H21(2)

2013), and Assemble Species by Automatic Partitioning (ASAP; Puillandre et al. 2020). We calculated pairwise distances in Mega under the K80 model (100 bootstraps, pairwise deletion of gaps; Kimura 1980). For GMYC, we built an ultrametric tree using BEAST 2.6.3 and BEAUTI for parameter settings (GTR+G+I as substitution model, a strict clock model, Yule model as prior). Analysis was run with 10,000,000 chains, whereof every 10,000th tree was stored. We set the burn-in to 25,000. The resulting 10,001 trees were further compiled with TreeAnnotator 2.6.3 (Bouckaert et al. 2019) to a maximum clade credibility tree with common ancestor heights by defining a burn-in of 10% and a posterior probability limit of 0.9. This final tree was then used for GMYC (single threshold version) using the R packages Paran (Dinno 2009; software retrieved from http://cran.r-project.org/web/, accessed

30 July 2022), Splits (Ezard et al. 2009; http://R-Forge.R-project.org/projects/splits/, accessed 30 July 2022), Mass (Ripley et al. 2015; software retrieved from http://cran.r-project.org/web/, accessed 30 July 2022), and Ape 5.0 (Paradis & Schliep 2019; software retrieved from http://cran.r-project.org/web/, accessed 30 July 2022). As a third species delimitation method, we created species partitions from single locus sequence alignments on the ASAP web server (https://bioinfo.mnhn.fr/abi/public/asap/asapweb.html, accessed 24 June 2021), with 'P' between 0.001 and 0.1; X = 0.5; N = 10 and K80 as substitution model, with ts/tv = 11.55 (transition/transversion ratio, according to the AICc results; see below).

Phylogenetic analyses

To test for monophyly of *A. trivittata* samples (goal 1B), we performed Bayesian Inference (BI) and Maximum Likelihood (ML) phylogenetic reconstructions. As outgroups we used *Ameerega braccata*, *A. picta* and *Colostethus pratti*, based on the topologies of Guillory et al. (2020). Outgroup sequences were obtained from GenBank (accession numbers: DQ502125, KJ940455, KR863143). We ran BI analyses in MrBayes 3.2.7 (Ronquist & Huelsenbeck 2003) with 100 million generations and two independent runs starting from different random trees, using the GTR+I+G substitution model. Chains were sampled every 10,000 generations. Convergence between the two runs was checked in Tracer 1.7.1 (Rambaut et al. 2018). The first 25% of the trees obtained were rejected as burn-in and the remaining sampled trees were used for building a consensus tree and estimation of Bayesian posterior probabilities (BPP). ML analyses were performed with IQtree 2.1.2 (Nguyen et al. 2015) under the TPM2uf+I+G model. Tree node support was assessed with 10,000 ultrafast bootstrap (UFBoot) replicates (Minh et al. 2013). For both analyses, base frequencies, proportion of invariable sites and gamma distributed rates were adopted according to the results of AICc.

Haplotype diversity

Goal (1C) was to test for signal of recent invasions into different directions by studying haplotype diversity. Genetic diversity parameters were computed with DnaSP including the number of polymorphic sites (S), nucleotide diversity (π), haplotype diversity (Hd) and mean number of nucleotide difference (K). Furthermore, we analyzed with DnaSP haplotype difference and the ratio of transitions and transversions. For intraspecific gene genealogies, we analyzed the phylogenetic relationships between sequences by creation of a haplotype network as follows. A statistical parsimony network was created in TCS 1.23 (Posada & Crandall 2000), with the 98% criterion for a parsimonious connection, then visualized with tcsBU (Múrias dos Santos et al. 2016).

Evolutionary biogeographical reconstruction

To test for early vicariance events in the Late Miocene and subsequent dispersal of *A. trivittata* (goal 2), we used a dated phylogeny and biogeographic modelling, similar to Réjaud et al. (2020).

Time-Calibrated Population Phylogeny. – To estimate the intraspecific diversification through time, we conducted a dated phylogeny using BEAST and BEAUTI for defining parameters (Bouckaert et al. 2019). There are no fossil records for dendrobatoids and their ancestors available, which prevents the possibility of a primary calibration of the molecular clock. We therefore applied a secondary calibration derived from Guillory et al. (2020). These authors estimated the split of *Ameerega* and *Colostethus* to 21.797 Mya with σ = 3.071 Mya, based on divergence time estimations with a fossil record background for the entire class of Amphibia as described in Santos et al. (2009). We used the estimated divergence times of the three-striped poison frog from its three close phylogenetic relatives (according to Guillory et al. 2020), *Ameerega picta* at 7.567 Mya with σ = 1.634 Mya, *A. braccata* at 9.252 Mya with σ = 1.846 Mya, and *Colostethus pratti* at 23.325 Mya with σ = 3.071 Mya as calibration points. Again the TPM2uf+I+G substitution model was employed. Further substitution parameters were set to four gamma rate categories with a fixed value for gamma shape and a proportion invariant as defined by JModeltest. We set a relaxed log-normal clock model with a clock rate prior of 1e-10 and a Yule tree model with default settings, as endorsed by Guillory et al. (2020). We ran three independent chains of 100,000,000 iterations with different random seeds. Trees were logged every 10,000 steps and the first 1,000,000 chains were ignored as pre-burn-in. ESS (effective sample size) values were controlled in Tracer and were above the recommended threshold of 200. The three runs were combined with LogCombiner 2.6.3 (Bouckaert et al. 2019) and summarized with TreeAnnotater using a maximum clade credibility tree and mean node heights with 10% burn-in.

Modelling. – A reliable method that combines phylogenetic data and geographic data to describe biogeographical events is the R package BioGeoBEARS of Matzke (2013). We accomplished ancestral area reconstruction and biogeographical event estimations under BI and ML frameworks in BioGeoBEARS. Here, the molecular clock tree obtained from BEAST served as an input. Our sampling contained various haplotypes from the same population, which can bias the results in BioGeoBEARS (N. Matzke, in litt. 19 August 2022). We therefore carefully pruned our tree to a meaningful population tree, using the pruning skript "How (and whether) to collapse tips to prune a tree" on PhyloWiki (http://phylo.wikidot.com/example-biogeobears-scripts#pruning_a_tree, accessed 28 August 2022). Moreover, we followed the recommendations of recent studies (e.g. Pirani et al. 2020, Réjaud et al. 2020, Fouquet et al. 2021a, b) and compared AICc values of a dispersal extinction cladogenesis model, representing vicariance and in situ diversification (DEC; cf. Ree & Smith 2008), a

likelihood version of the dispersal vicariance model which stands for a majority of vicariance events (DIVALIKE; cf. Ronquist 1997), and a likelihood version of the BayArea model, preferred for the majority of in situ diversification (BBM; cf. Landis et al. 2013). We also followed the cautionary advice of Ree & Sanmartin (2018) and did not include jump dispersal parameters, as these can enlarge cladogenetic events to the detriment of anagenetic events and time-dependent range evolution. Following Dupin et al. (2017), we conducted 100 independent runs of biogeographical stochastic mapping (BSM) in BioGeoBEARS to determine biogeographical event counts for the best-fitting model.

To finally reconstruct processes at different spatio-temporal scales, we allocated sample localities of *A. trivittata* into the BRs (Fig. 1). According to Godinho & Silva (2018), these BRs well reflect the regionalization of anuran dissimilarity in Amazonia. The spatial clustering into BRs allowed us to investigate potential dispersal events of our study species during the diversification of the Amazon basin and the establishment of the Amazon River system from the Acre system over the last ca. 9 Ma (cf. Vacher et al. 2017). We allowed for the three models mentioned above a maximum of six reconstructed areas per node, which equals an occupation of all BR groups where *A. trivittata* occurs.

Results

Species delimitation, phylogeny and genetic diversity

The comparison of the uncorrected p-distances and GMYC suggested within-species variation. In contrast, ASAP delimited two groups suggesting the possible presence of two taxa under the name *A. trivittata*. In detail, the uncorrected p-distances revealed genetic variation at ≤ 2.3%, with most values < 2% (Supplementary Table S2). Taking the rule-of-thumb threshold of 5% for anuran species delimitation in this fragment of the 16S rRNA gene (fide Vences et al. 2005b), our *A. trivittata* samples rather represent conspecifics. Under the GMYC model, all *A. trivittata* haplotypes were delimited into three clusters (Supplementary Table S3). However, there was no geographic signal, and the likelihood ratio test was not significant (LR test = 0.097), indicating that our *A. trivittata* dataset belongs to a single species. In contrast, the ASAP analysis revealed two groups, i.e. potential taxa, with an 'ASAP score' of 4.00, a P-val rank of 0.93 and a threshold distance of 0.00729. These two groups comprised: (i) three haplotypes from five localities along the Madeira River: Castanho (H1), Humaita (H19), Ilha da Pedra (H1, H16), Ilha do Bufalo (H1) and Teotônio (H1) (Figs 1, 2); (ii) all other samples including those from the type locality (Rio Tefé, Estado Amazonas, Brazil).

Both phylogenetic trees (BI: Fig. S1; ML: Fig. S2) support the monophyly of *A. trivittata*. In concert with the ASAP results and the haplotype network, samples of the Madeira River group are defined as a sister clade to all other *A. trivittata* with robust support (BI: BPP = 100; ML: UFBoot = 91).

Table 2. Genetic diversity of *Ameerega trivittata* haplotypes found in the respective biogeographic regions (BR) with N = number of samples; h = number of haplotypes; S = number of polymorphic sites; π = nucleotide diversity; Hd = haplotype diversity and K = mean number of differences.

BR	N	h	S	Π	Hd	K
BR1	13	10	12	0.00848	0.949	4.103
BR2	3	1	0	0	0.000	0.000
BR4	27	14	13	0.00577	0.934	2.758
BR5	6	4	4	0.00387	0.867	1.867
BR6	5	3	7	0.00579	0.700	2.800
BR7	3	3	8	0.01102	1.000	5.333
all BRs	57	36	26	0.00829	0.966	3.955

The 36 unique haplotypes (108 samples; Tab. 1) differed at 26 polymorphic sites with 10 singletons and 16 parsimony informative sites and showed ts/tv = 11.55. Haplotype diversity and nucleotide diversity of all identified haplotypes were relatively high (Hd = 0.966; Pi = 0.829%). Haplotype diversity varied across sample sites and biogeographic regions (Tab. 2). The maximum number of haplotypes at one locality was six (Panguana, at the same time the locality with the highest samples size); the most common haplotype (H3) was recorded at five localities (Tab. 1). The haplotype network shown in Figure 2a revealed a 'star burst' pattern for samples from western and central Amazonia (BR1, BR4, BR5). Genetically most distant from the star burst were the haplotypes from regions BR2, BR6 and BR7. In addition, the haplotypes of the Madeira River group (H1, H16, H19) from regions BR6 and BR7 formed a cluster that was not connected to the other haplotypes (Fig. 2a, b).

Within-species evolution and biogeography

In the independent BEAST runs, the *A. trivittata* samples were discriminated further (Fig. S3) resulting in (1) the Madeira River group, (2) a Northeastern central Amazonian group, (3) a Western central and southern Amazonian group. These splits were supported by BPP = 0.972 and 0.902, respectively. Our time estimation dated the diversification of *A. trivittata* from its sister *A. picta* at 8.44 Mya (95% HPD: 10.6–6.04 Mya). *Ameerega trivittata* split further at 6.87 Mya (95% HPD: 9.2–4.55 Mya), representing the basal split of the Madeira River group from groups (2) and (3). At 5.75 Mya (95% HPD: 7.91–3.56 Mya), the last two mentioned groups split.

Comparisons of the BioGeoBEARS models AICc identified DIVALIKE as the best-fit model (Tab. 3). Our area reconstruction revealed that the most likely ancestral estimated area of *A. trivittata* was composed of BR1, BR4, BR5 and BR6 (Fig. 3). Moreover, biogeographical stochastic mapping suggested that the segregation of the principal

groups (1) to (3) is best explained by vicariance events (V1 around 6.87 Mya and V2 around 5.75 Mya; Fig. 3). BioGeoBEARS suggested an additional vicariance event within group (3), which segregates a geographic unit comprised by (A) the southern Amazonian samples from (B) the western central Amazonian samples (V3 around 5 Mya; Fig. 3). However, this split received no support in the BEAST topology (Fig. S3). Subsequent within-group diversification, younger than circa 5 Mya, was identified to be best explained by dispersal events.

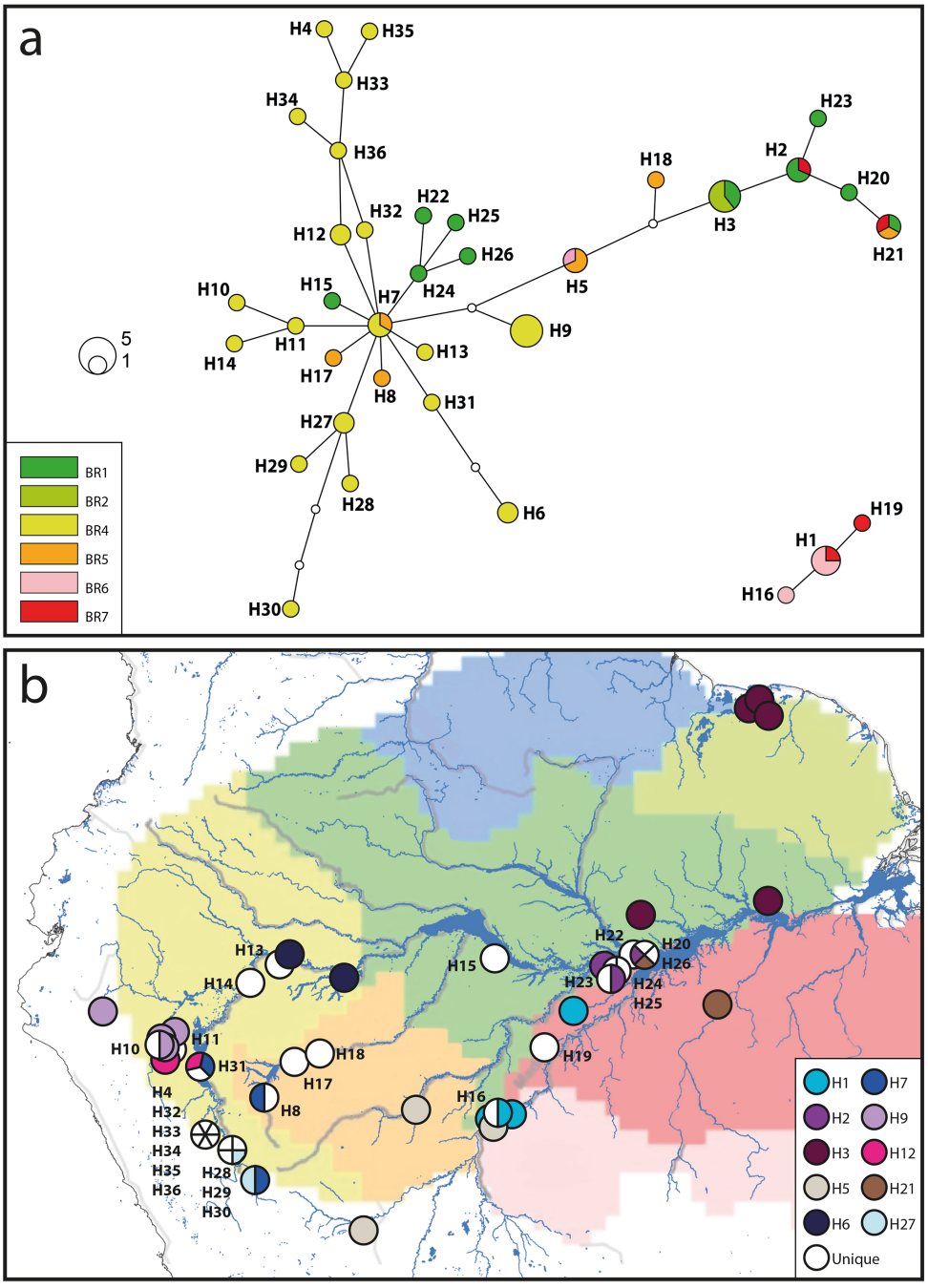

Figure 2. Haplotypes of *Ameerega trivittata*: (a) Statistical parsimony network pattern (98%) inferred from the 36 haplotypes from 38 localities, with the Madeira River group (H1, H16, H19, see text) showing a separate network (using a 95% parsimony limit: H1 connects to H3, H5, H7 with five mutations; H19 connects to H6 with five; H16 connects to H6 via H19 with six mutations – not shown). Colors are according to BR allocation (Fig. 1, Tab. 1); the number of samples per haplotype is indicated by circle size on the left margin. (b) Map of northern South America showing the distribution of the unique and the most shared haplotypes (faded background colors are those of BRs in Fig. 1).

Table 3. BioGeoBears AICc results. Abbreviations: LnL = ln(likelihood); d = dispersal; e = extinction; j = founder-event speciation.

Model	LnL	d	e	j	AICc	AICc_wt
DEC	-63.7359	0.0152	1.0e-12	0	131.7718	5.2994
DIVALIKE	-59.0920	0.0207	1.0e-12	0	122.4839	5.5088
BAYAREALIKE	-80.5670	0.0112	0.2852	0	165.4340	2.5976

Discussion

Hypotheses testing

Our results demonstrate low genetic divergence among (uncorrected p-distances, GYMC, but not ASAP, as discussed below) and monophyly (BI and ML) of *A. trivittata* samples as well as multidirectional 'star burst' dispersal of extant haplotypes. The biogeographic modelling suggest three vicariance events before 5 Mya and multiple dispersal events in more recent times. Thus, the expectations formulated above (cf. goals 1A–C; 2) are supported.

The observed low genetic diversity over Amazonia markedly differs from many other widespread Amazonian anurans that have been studied in detail in recent years and that turned out to be complexes of species with relatively small allopatric distributions (e.g. Padial & De la Riva 2009, Angulo & Icochea 2010, Funk et al. 2012, Fouquet et al. 2014, 2021b, Gehara et al. 2014, Peloso et al. 2014, Rojas et al. 2018, Réjaud et al. 2020). Notable in this context is the ASAP result that revealed the existence of two lineages that could represent distinct taxa in our *A. trivittata* sampling. In this case, a small fraction of samples comprising the Madeira River group (from 5 localities with 3 unique haplotypes, Fig. 2) would specifically differ from all other *A. trivittata* samples. However, this is not supported by the relatively low p-distances (≤ 0.023;

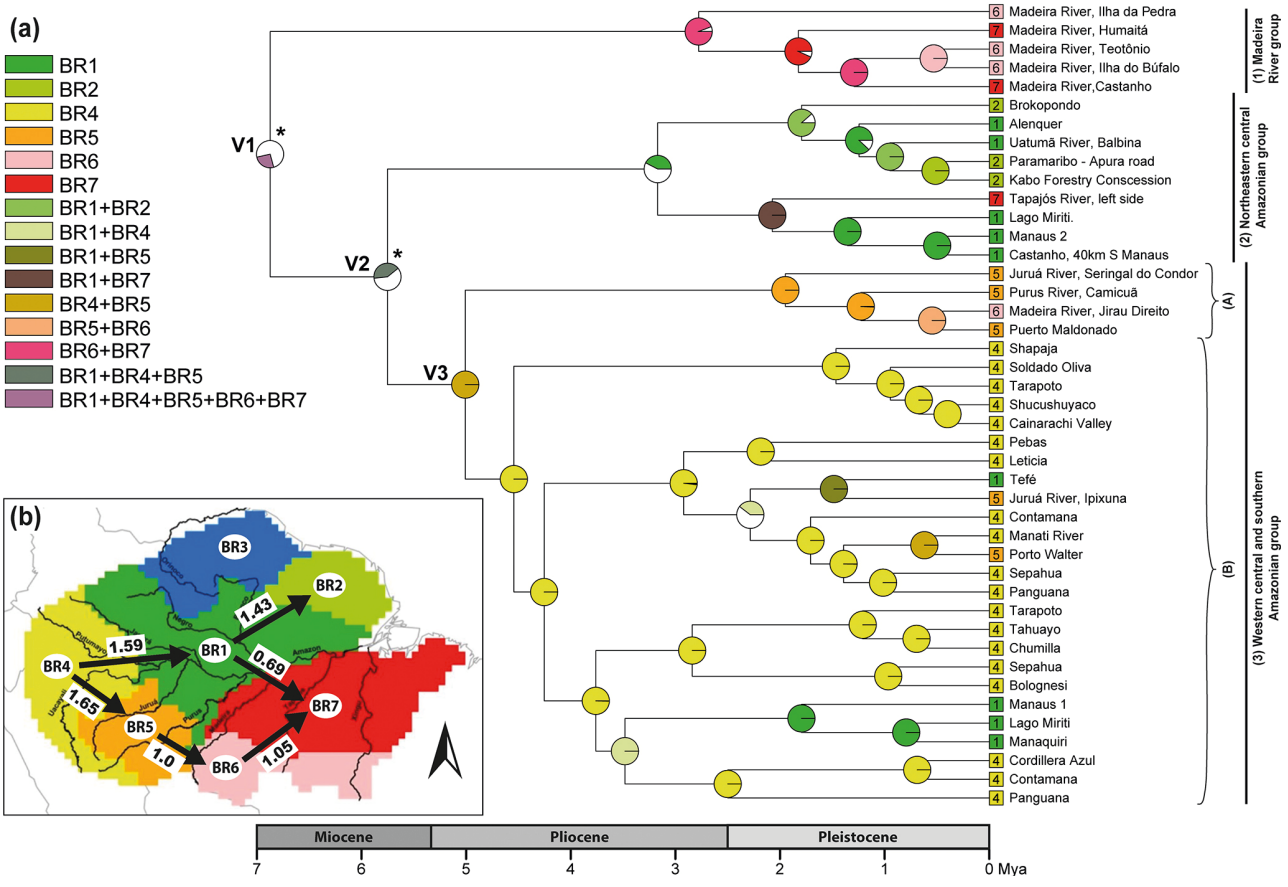

Figure 3. Ancestral area reconstruction of the three-striped poison frog, *Ameerega trivittata,* inferred in BioGeoBEARS under the best-fit DIVALIKE model, with: (a) the most likely biogeographic scenario, with pie charts at nodes displaying the probability of the ancestral estimated areas in colors and less likely estimations in white. Colors correspond to the BR as indicated on the left margin. Vicariance events are V1 to V3, while all other splits represent dispersal events. Group names as in text. (b) Map of Amazonia with the seven BRs and biogeographical stochastic mapping (BSM) with anagenetic dispersal events; numbers indicate mean range-expansion dispersal events and are shown with a mean of > 0.6 only. Note that only basal nodes received robust support (*), see text.

Supplementary Table S2) that rather suggest conspecificy (cf. Vences et al. 2005b).

Intraspecific gene genealogies indicated a high haplotype diversity (Hd = 0.966), and several identical haplotypes were recorded from different localities (Fig. 2b). These data, in combination with the relatively high ts/tv ratio (11.55), suggest a recent evolutionary history and interchange of populations. This is also supported by the 'star burst' pattern of the parsimony network for samples from western and central Amazonia (BR1, BR4, BR5), implying this region to be a dispersal center for our study species. In line with this, haplotypes associated with localities in the periphery of Amazonia (BR2, BR6, BR7) were genetically fairly distant. These findings propose that *A. trivittata* invaded into these localities. In conclusion, the intraspecific gene genealogies well match the hypothesis of a recent within-species evolution.

Not only the haplotype network, but also the molecular clock and the biogeographic modelling support that the many younger splits in the *A. trivittata* phylogeny (< ca. 4.5 Mya) are likely the result of relatively recent forward and backward dispersal events among BRs. Only prior to that, in the Late Miocene, largely between 7 and 5 Mya, vicariance was apparently a major driver for within-species segregation. Stochastic mapping revealed that these early splits have taken place in western to central Amazonia (BR1, BR4, BR5, BR6). We find support for a phylogeographic scenario that (i) with the formation of the young Amazon River and the retention of enormous water masses in the Late Miocene (Hoorn et al. 2010, Shephard et al. 2010), *A. trivittata* underwent vicariance events. (ii) When later, around 3 Mya, water bodies burst into the Amazon River and diminished, *A. trivittata* was able to disperse between BRs and to expand its geographic range through invasion into the periphery of the Amazon basin.

Translation into hypothetical phylogeographic scenarios

Our results are consistent with geological and landscape diversification processes of the Amazon basin of the last 10 million years. During this period, central Amazonia changed from the lacustrine Acre System gradually into the modern Amazon watershed with an expansion of terra firme forests (Hoorn et al. 2010). Enabled by the uplift of the Andes, the drainage of these lacustrine accumulations and influxes, which formed the early stages of the Amazon River, was able to breach the Purus Arch around 10.1–8.3 Mya (Shephard et al. 2010, Gorini et al. 2014, Albert et al. 2018). The formation of the Amazon basin obviously was a major geodispersal event with predictable consequences for biodiversity, despite that rivers were not the only drivers of species diversification in Amazonia (Cracraft et al. 2020). As figured out by Hoorn et al. (2010), these changes in the landscape played a decisive role in the evolutionary and biogeographic history of Amazonian plant and animal biodiversity.

The three-striped poison frog emerged in this time (8.44 Mya; 95% HPD: 10.6–6.04 Mya; Fig. S3), which is not only supported by our time estimations but also by those of other authors (Santos et al. 2009, Guillory et al. 2020). According to Santos et al. (2009), *A. trivittata* is of Amazonian origin in the vicinity of the remnant of the former Pebas System. We propose that like other contemporary biota (Réjaud et al. 2020, Fouquet et al. 2021a), north and south of the remnant of the Acre System, it colonized continuous terra firme forest in central Amazonia via the opening of the Purus Arch (Fig. 4a, b). However, we can only assume this here because of vicariance events – a result of our biogeographic modelling – that took place later.

Since the Late Miocene (11.6–5.3 Mya), the Andes in the West more and more attained their present shape. Only since then, the formation of the Amazon basin as presently known began. The establishment of the transcontinental Amazon River and the arrangement of its tributaries took until about 4.5 Mya (Gorini et al. 2014, Albert et al. 2018) or even longer (Shephard et al. 2010). Rivers that initiated through the continuous Andean uplift and today are known as major tributaries of the Amazon, for longer periods were enormous water accumulations, because the Purus Arch in central Amazonia had not entirely eroded. Our findings of early vicariance scenarios (Fig. 3a) suggest that at least three of these arising water catchments represented temporary riverine barriers to *A. trivittata*.

One vicariance event (V1) that took place around 6.87 Mya coincides well with river captures of the Upper Madeira basin (Fig. 4c) (Albert et al. 2018, Cooke et al. 2012, Tagliacollo et al. 2015). Another vicariance event (V2) noted in *A. trivittata* occurred at around 5.75 Mya. It can well be linked to the emergence of the Negro River (Fig. 4d). This water catchment resulted from the turn of the Branco River, which originally drained north into the Caribbean Sea via the Essequibo River (Albert et al. 2018). It then had become an enormous water catchment for about 1–2 Mya north of the Amazon River (Almeida-Filho & Miranda 2007, Ribas et al. 2012). The Negro River had acted as a barrier for various taxa, including primates or even birds (d'Horta et al. 2013, Boubli et al. 2015). While the water retention of the young Negro River might have represented a riverine barrier to *A. trivittata*, we find no signal that the lower Amazon River was impermeable to this species. At least, Lougheed et al. (1999) showed that for extant populations of *Allobates femoralis*, another Amazonian terra firme poison frog, the Juruá River is not a barrier, which perhaps is about the same size as was the lower Amazon River at about 6 Mya.

The three putative isolates of *A. trivittata* remained with the complete dissolvement of the Acre System. Afterwards, with the forebulge of the Fitzcarrald Arch at about 5 Mya, geomorphology and drainage systems in the South of the upper Amazon basin massively re-shaped, including a shift of the upper Amazon (Solimões) River to the North (Espurt et al. 2010). The Juruá and Purus Rivers might then have turned into barriers to *A. trivittata,* corresponding to a possible third vicariance (V3) event at around 5 Mya (Fig. 4e).

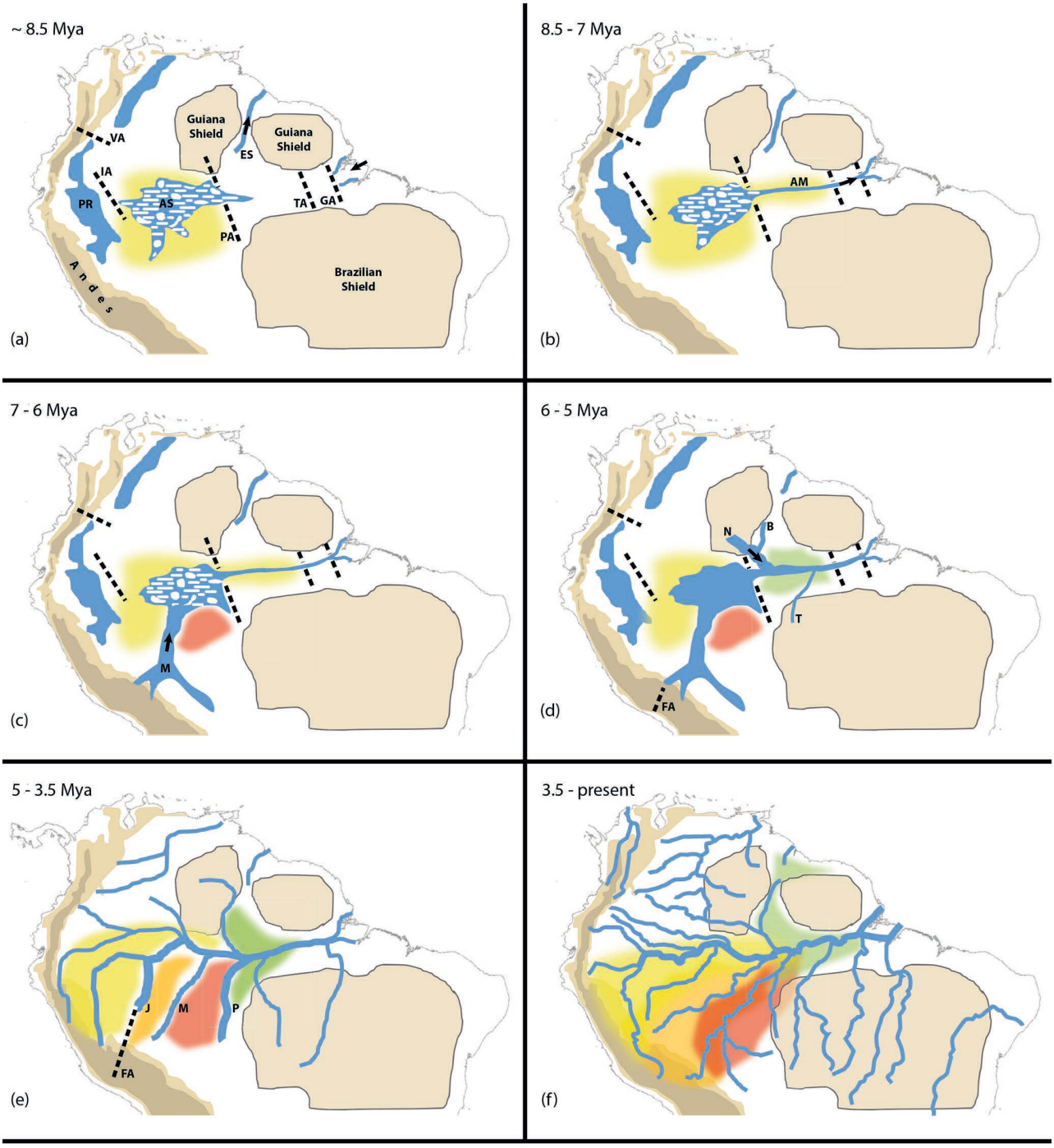

PR	= Pebas Remnant	PA	= Purús Arch	ES	= Esequibo River	B	= Branco River
AS	= Acre System	TA	= Tapajós Arch	AM	= Amazonas River	T	= Tapajos River
VA	= Vaupes Arch	GA	= Gurupá Arch	M	= Upper Madeira River	J	= Juruá River
IA	= Iquitos Arch	FA	= Fitzcarrald Arch	N	= Negro River	P	= Purus River

Figure 4. Hypothetical biogeographic history of the three-striped poison frog, characterized by three vicariance events through river barriers, indicated by yellow, red, green and orange colors. Main mountains (tan), ancient arches (stipples) and water bodies (blue) are shown, with arrows indicating flow direction. Underlying is a map of extant northern South America. Main rivers are adopted from illustrations in Albert et al. (2018) and Hoorn et al. (2010).

For the last 3.5 Mya, the landscapes of the Amazon basin have not undergone drastic changes anymore, only rivers slimed down at some extent (Hoorn et al. 2010) so that apparently *A. trivittata* was able to cross them and to expand its geographic range further (e.g. into the Guianas), exhibiting its extant pan-Amazonian distribution (Fig. 4f).

Dispersal advantages as a key explanation

When trying to understand the evolutionary biogeography of Amazonian taxa, species' intrinsic characteristics, including dispersal ability and niche breadth are pivotal (e.g. Pirani et al. 2019, Fouquet et al. 2021b). Our data infer that *A. trivittata* once it has expanded its range into central Amazonia (similar to other anurans; e.g. Santos et al. 2009, Réjaud et al. 2020), riverine barriers had a lesser effect on this species than on other anurans, so that time of segregation was too short to evolve irreversible reproductive isolation (lineages). Afore mentioned species-specific characteristics may have played a key role here, and we suggest that the three-striped poison frog exhibits life history traits that make it a more successful disperser than other anurans.

First, as mentioned above, *A. trivittata* is one of the largest poison frog species. Its maximum adult size is about one third larger than that of *Allobates femoralis* sensu lato (Silverstone 1976, Lötters et al. 2007), and thus, *A. trivittata* is larger than many other Amazonian anurans (see Oliveira et al. 2017). In anurans, larger body size favors dispersal (Wollenberg et al. 2011, Searcy et al. 2018). Moreover, larger amphibian species commonly have a higher body mass and can better cope with unfavorable conditions compared to smaller species (Duellman & Trueb 1986). This may upsurge survival rates in accidental long distance dispersal over rivers known in anurans (cf. Marin da Fonte et al. 2019). Such an event, although probably rare, was reported in the Amazonian poison frog *Ameerega hahneli* (Montanarin et al. 2017). It is smaller than *A. trivittata*, so that long distance dispersal success, undergoing potential fluviatile drift, should even be higher in the larger *A. trivittata.*

Dispersal success in *A. trivittata* is additionally stimulated by its diurnal and terrestrial life style (Lötters et al. 2007, Kahn et al. 2016). Most Amazonian anurans are nocturnal so that in this region mainly poison frogs cover this general niche; they are all smaller than *A. trivittata* (Montanarin et al. 2017). An exception is *Ameerega bassleri*, co-occurring with *A. trivittata* along the lower Andean versant in Peru (i.e. *A. bassleri* does not emerge into lowlands). It is about the same size and clearly outcompetes *A. trivittata* (Twomey et al. 2008). In other sites, where various poison frog species occur in syntopy, *A. trivittata* is the most common one (Schlüter 2005; authors' unpubl. data), suggesting that probably it better asserts itself along limiting niche axes.

Other aspects increasing the dispersal ability of *A. trivittata* can be linked to particular behavioral traits of parental care. Poison frogs actively promote offspring dispersal by carrying their larvae to water bodies over relatively large distances (Pašukonis et al. 2019). We propose that the length of this transport way is positively correlated with adult size and that *A. trivittata* performs active offspring dispersal over larger distances than smaller poison frogs. At least, Pašukonis et al. (2019) demonstrated that this species carries its tadpoles for up to 300 m away from its home range (comparative data for other taxa are sparse). Moreover, *A. trivittata* is one of the poison frog species with the highest number of eggs, probably also a result of its large size. It is known to lay up to about 50 eggs in one clutch (inferred from one male transporting 46 tadpoles and one female having 51 ovarian eggs; Aichinger 1991). Known maximum clutch size in other *Ameerega* species is considerably less, mostly < 20 (Aichinger 1991, Lötters et al. 2007). Anuran clutch size is positively correlated with dispersal ability (Trakimas et al. 2016), and it has been shown to represent an important aspect in a dispersal study on West African amphibians (Penner & Rödel 2019). Compared to other anurans, for instance explosive breeders, clutch size in *A. trivittata* is 'tiny'. However, in combination with the species' brood care behavior including active offspring dispersal, dispersal via reproduction may be quite effective in it.

Future research

Poison frogs are an important group with regard to understanding Amazonian biogeography (Santos et al. 2009). Our results suggest that one member of this group, *A. trivittata,* represents an extraordinary case, because it encompasses a truly pan-Amazonian distribution. Despite that we have an incomparable spatial sampling and provide an explanatory phylogeographic scenarios, at the same time the accuracy of our study is limited by the use of only one mtDNA marker and with a varying number of samples per locality. Moreover, some questions remain unanswered, especially those concerning spatial processes in more recent times (≤ 3.5 Mya). The use of nuclear genomic data might provide a clearer picture and provide results beyond ours. However, the availability of materials is challenging and gathering nuDNA data for all the terminals included in our study was out of reach, so that our study is best be seen as a frame for a future approach (cf. Réjaud et al. 2020). Future research might also aim to better emphasize the dispersal advantages that we suggest *A. trivittata* has compared to other poison frogs.

Conclusion

The evolutionary biogeography of pan-Amazonian anuran taxa is little understood. We, for the first time, show that recent (Pliocene/Pleistocene) multidirectional dispersal plays a role, using the three-striped poison frog, *A. trivittata*, as a case study. Due to its intrinsic morphological and life history traits it is a more successful disperser than other anuran species, so rivers are more permeable.

Acknowledgements

For help with obtaining samples, we thank S. Bisanz, M. Chouteau, A. De Lima, R. Ernst, M. Ferrão, L. João, M. Juruna, L. F. Marin da Fonte, Philipe, Pinduca, Rato, Rubico, F. Rubio, L. M. Schulte, P. I. Simões and E. Twomey. Lab work was performed with support of P. Willems. Permits were kindly issued by SISBIO (Brazil), SERFOR (Peru) and national CITES authorities. Two anonymous reviewers made most valuable comments on the manuscript of this paper, and N. Matzke kindly provided helpful information on BioGeoBEARS. For support to the first author, we are indebted to the Konrad-Adenauer-Stiftung (KAS). We are especially grateful and we dedicate this paper to M. Menin† who contributed to the concept of this study and who helped carry out fieldwork in Brazil.

References

Aichinger, M. (1991): Tadpole transport in relation to rainfall, fecundity and body size in five species of poison-dart frogs from Amazonian Peru. – Amphibia-Reptilia, **12**: 49–55.

Albert, J. S., P. Val & C. Hoorn (2018): The changing course of the Amazon River in the Neogene: center stage for Neotropical diversification. – Neotropical Ichthyology, **16**: 1–23.

Almeida-Filho, R. & F. P. Miranda (2007): Mega capture of the Rio Negro and formation of the Anavilhanas Archipelago, central Amazônia, Brazil: evidences in an SRTM digital elevation model. – Remote Sensing of Environment, **110**: 387–392.

Angulo, A. & J. Icochea (2010): Cryptic species complexes, widespread species and conservation. Lessons from Amazonian frogs of the *Leptodactylus marmoratus* group (Anura: Leptodactylidae). – Systematics and Biodiversity, **8**: 357–370.

Antonelli, A., A. Zizka, D. Silvestro, R. Scharn, B. Cascales-Miñana & C. D. Bacon (2015): An engine for global plant diversity: highest evolutionary turnover and emigration in the American tropics. – Frontiers in Genetics, **6**: 130.

Antonelli, A., A. Zizka, F. A. Carvalho, R. Scharn, C. D. Bacon, D. Silvestro & F. L. Condamine (2018): Amazonia is the primary source of Neotropical biodiversity. – Proceedings of the National Academy of Sciences, **115**: 6034–6039.

Benson, D. A., K. Clark, I. Karsch-Mizrachi, D. J. Lipman, J. Ostell & E. W. Sayers (2015): GenBank. – Nucleic Acids Research, **43**: D30.

Bouckaert, R., T. G. Vaughan, J. Barido-Sottani, S. Duchêne, M. Fourment, A. Gavryushkina, J. Heled, G. Jones, D. Kühnert, N. de Maio, M. Matschiner, F. K. Mendes, N. F. Müller, H. A. Ogilvie, L. du Plessis, A. Popinga, A. Rambaut, D. Rasmussen, I. Siveroni, M. A. Suchard, C.-H. Wu, D. Xie, C. Zhang, T. Stadler & A. J. Drummond (2019): BEAST 2.5: An advanced software platform for Bayesian evolutionary analysis. – PLoS Computational Biology, **15**: e1006650.

Boubli, J. P., C. Ribas, J. W. L. Alfaro, M. E. Alfaro, M. N. F. da Silva, G. M. Pinho & I. P. Farias (2015): Spatial and temporal patterns of diversification on the Amazon: a test of the riverine hypothesis for all diurnal primates of Rio Negro and Rio Branco in Brazil. – Molecular Phylogenetics and Evolution, **82**: 400–412.

Brown, J. L., E. Twomey, A. Amezquita, M. B. De Souza, J. P. Caldwell, S. Lötters, R. von May, P. R. Melo-Sampaio, D. Mejia-Vargas, P. Perez-Peña, M. Pepper, E. H. Poelman, M. Sanchez-Rodriguez & K. Summers (2011): A taxonomic revision of the Neotropical poison frog genus *Ranitomeya* (Amphibia: Dendrobatidae). – Zootaxa, **3083**: 1–120.

Buckley, L. B. & W. Jetz (2007): Environmental and historical constraints on global patterns of amphibian richness. – Proceedings of the Royal Society B: Biological Sciences, **274**: 1167–1173.

Cracraft, J., C. C. Ribas, F. M. d'Horta, J. Bates, R. P. Almeida, A. Aleixo, J. P. Boubli, K. E. Campbell, F. W. Cruz, M. Ferreira, S. C. Fritz, C. H. Grohmann, E. M. Latrubesse, L. G. Lohmann, L. J. Musher, A. Nogueira, A. O. Sawakuchi & P. Baker (2020): The origin and evolution of Amazonian species diversity. – pp. 225–244 in: Rull, V. & C. Carnaval (eds): Neotropical diversification: patterns and processes. – Cham etc.: Springer.

Castresana, J. (2000): Selection of conserved blocks from multiple alignments for their use in phylogenetic analysis. – Molecular Biology and Evolution, **17**: 540–552.

Castroviejo-Fisher, S., J. Köhler, I. De La Riva & J. M. Padial (2017): A new morphologically cryptic species of *Phyllomedusa* (Anura: Phyllomedusidae) from Amazonian forests of northern Peru revealed by DNA sequences. – Zootaxa, **4269**: 245–264.

Collevatti, R. G., L. Leoi, S. A. Leite & R. Gribel (2009): Contrasting patterns of genetic structure in *Caryocar* (Caryocaraceae) congeners from flooded and upland Amazonian forests. – Biological Journal of the Linnean Society, **98**: 278–290.

Cooke, G. M., N. L. Chao & L. B. Beheregaray (2012): Marine incursions, cryptic species and ecological diversification in Amazonia: the biogeographic history of the croaker genus *Plagioscion* (Sciaenidae). – Journal of Biogeography, **39**: 724–738.

Darriba, D., G. L. Taboada, R. Doallo & D. Posada (2012): jModelTest 2: more models, new heuristics and parallel computing. – Nature Methods, **9**: 772.

d'Horta, F. M., A. M. Cuervo, C. C. Ribas, R. T. Brumfield & C. Y. Miyaki (2013): Phylogeny and comparative phylogeography of *Sclerurus* (Aves: Furnariidae) reveal constant and cryptic diversification in an old radiation of rain forest understory specialists. – Journal of Biogeography, **40**: 37–49.

Dinno, A. (2009): Exploring the sensitivity of Horn's parallel analysis to the distributional form of simulated data. – Multivariate Behavioral Research, **44**: 362–388.

Duellman, W. E. & L. Trueb (1994): Biology of amphibians. – New York etc., McGraw-Hill.

Dupin, J., N. J. Matzke, T. Särkinen, S. Knapp, R. G. Olmstead, L. Bohs & S. D. Smith (2017): Bayesian estimation of the global biogeographical history of the Solanaceae. – Journal of Biogeography, **44**: 887–899.

Edgar, R. C. (2004): MUSCLE: multiple sequence alignment with high accuracy and high throughput. – Nucleic Acids Research, **32**: 1792–1797.

Espurt, N., P. Baby, S. Brusset, M. Roddaz, W. Hermoza & J. Barbarand (2010): The Nazca Ridge and uplift of the Fitzcarrald Arch: implications for regional geology in northern South America. – pp. 89–100 in: Hoorn, C. & F. Wesselingh (eds): Amazonia: landscape and species evolution: a look into the past. – Chichester, Wiley-Blackwell.

Ezard, T., T. Fujisawa & T. Barraclough (2009): SPLITS 1.0-20 – Species limits by threshold statistics. R package, version

1.0-18/r45. Available from: http://R-Forge.R-project.org/projects/splits, accessed 30 July 2022.

Fouquet, A., A. Gilles, M. Vences, C. Marty, M. Blanc, N. J. Gemmell & J.-N. Volff (2007): Underestimation of species richness in Neotropical frogs revealed by mtDNA analyses. – PLoS ONE, **2**: e1109.

Fouquet, A., R. Recoder, M. Teixeira Jr, J. Cassimiro, R. C. Amaro, A. Camacho, R. Damasceno, A. C Carnaval, C. Moritz & M. T. Rodrigues (2012): Molecular phylogeny and morphometric analyses reveal deep divergence between Amazonia and Atlantic Forest species of *Dendrophryniscus*. – Molecular Phylogenetics and Evolution, **62**: 826–838.

Fouquet, A., C. Cassini, C. F. B., Haddad, N. Pech & M. T. Rodrigues (2014): Species delimitation, patterns of diversification and historical biogeography of a Neotropical frog genus; *Adenomera* (Anura, Leptodactylidae). – Journal of Biogeography, **41**: 855–870.

Fouquet, A., K. Leblanc, M. Framit, A. Réjaud, M. T. Rodrigues, S. Castroviejo-Fisher, P. L. V. Peloso, I. Prates, S. Manzi , U. Suescun, S. Baroni, L. J. C. L. Moraes, R. Recoder, S. M. De Souza, F. Dal Vecchio, A. Camacho, J. M. Ghellere, F. J. M. Rojas-Runjaic, G. Gagliardi-Urrutia, V. T. De Carvalho, M. Gordo, M. Menin, P. J. R. Kok, T. Hrbek, F. P. Werneck , A. J. Crawford, S. R. Ron, J. J. Mueses-Cisneros, R. R. R. Zamora, D. Pavan, P. I. Simões, R. Ernst & A.-C. Fabre (2021a): Species diversity and biogeography of an ancient frog clade from the Guiana Shield (Anura: Microhylidae: *Adelastes, Otophryne, Synapturanus*) exhibiting spectacular phenotypic diversification. – Biological Journal of the Linnean Society, **132**: 233–256.

Fouquet, A., P. Marinho, A. Réjaud, T. R. Carvalho, M. A. Caminer, M., Jansen, R. N. Rainha, M. T. Rodrigues, F. P. Werneck, A. P. Lima, T. Hrbek, A. A. Giaretta, P. J. Venegas, G. Chávez & S. R. Ron (2021b): Systematics and biogeography of the *Boana albopunctata* species group (Anura, Hylidae), with the description of two new species from Amazonia. – Systematics and Biodiversity, **19**: 375–399.

Fujisawa, T. & T. G. Barraclough (2013): Delimiting species using single-locus data and the Generalized Mixed Yule Coalescent approach: a revised method and evaluation on simulated data sets. – Systematic Biology, **62**: 707–24.

Funk, W. C., J. P. Caldwell, C. E. Peden, J. M. Padial, I. De la Riva & D. C. Cannatella (2007): Tests of biogeographic hypotheses for diversification in the Amazonian forest frog, *Physalaemus petersi*. – Molecular Phylogenetics and Evolution, **44**: 825–837.

Funk, W. C., M. Caminer & S. R. Ron (2012): High levels of cryptic species diversity uncovered in Amazonian frogs. – Proceedings of the Royal Society B, Biological Sciences, **279**: 1806–1814.

Gehara, M., A. J. Crawford, V. G. Orrico, A. Rodríguez, S. Lötters, A. Fouquet, L. S. Barrientos, F. Brusquetti, I. De la Riva, R. Ernst, G. Gagliardi-Urrutia, F. Glaw, J. M. Guayasamin, M. Hölting, M. Jansen, P. J. R. Kok, A. Kwet, R. Lingnau, M. Lyra, J. Moravec, J. P. Pombal Jr, F. J. M. Rojas-Runjaic, A. Schulze, J. C. Señaris, M. Solé, M. T. Rodrigues, E. Twomey, C. F. B. Haddad, M. Vences & J. Köhler (2014): High levels of diversity uncovered in a widespread nominal taxon: continental phylogeography of the Neotropical tree frog *Dendropsophus minutus*. – PLoS ONE, **9**: e103958.

Grant, T., D. R. Frost, J. P. Caldwell, R. Gagliardo, C. F. Haddad, P. J. R. Kok, D. B. Means, B. P. Noonan, W. E. Schargel, & W. C. Wheeler (2006): Phylogenetic systematics of dart-poison frogs and their relatives (Amphibia: Athesphatanura: Dendrobatidae). – Bulletin of the American Museum of Natural History, **2006**: 1–262.

Grant, T., M. Rada, M. Anganoy-Criollo, A. Batista, P. H. Dias, A. M. Jeckel, D. J. Machado & J. V. Rueda-Almonacid (2017): Phylogenetic systematics of dart-poison frogs and their relatives revisited (Anura: Dendrobatoidea). – South American Journal of Herpetology, **12**: S1–S90.

Godinho, M. B. & F. R. Da Silva, (2018): The influence of riverine barriers, climate and topography on the biogeographic regionalization of Amazonian anurans. – Scientific Reports, **8**: 1–11.

Gorini, C., B. U. Haq, A. T. dos Reis, C. G. Silva, A. Cruz, E. Soares & D. Grangeon (2014): Late Neogene sequence stratigraphic evolution of the Foz do Amazonas Basin, Brazil. – Terra Nova, **26**: 179–185.

Guillory, W. X., M. R. Muell, K. Summers & J. L. Brown (2019): Phylogenomic reconstruction of the Neotropical poison frogs (Dendrobatidae) and their conservation. – Diversity, **11**: 126.

Guillory, W. X., C. M. French, E. Twomey, G. Chávez, I. Prates, R., von May, I. De la Riva, S. Lötters, S. Reichle, S. J. Serrano-Rojas, A. Whitworth & J: L. Brown (2020): Phylogenetic relationships and systematics of the Amazonian poison frog genus *Ameerega* using ultraconserved genomic elements. – Molecular Phylogenetics and Evolution, **142**: 106638.

Hill, J. L. & R. A. Hill (2001): Why are tropical rain forests so species rich? Classifying, reviewing and evaluating theories. – Progress in Physical Geography, **25**: 326–354.

Hoorn, C., F. P. Wesselingh, H. Ter Steege, M. A. Bermudez, A. Mora, J. Sevink, I. Sanmartín, A. Sanchez-Meseguer, C. L. Anderson, J. P. Figueiredo, C. Jaramillo, D. Riff, F. R. Negri, H. Hooghiemstra, J. Lundberg, T. Stadler, T. Särkinen & A. Antonelli (2010): Amazonia through time: Andean uplift, climate change, landscape evolution and biodiversity. – Science, **330**: 927–931.

Hoorn, C., G. R. Bogotá-A., M. Romero-Baez, E. I. Lammertsma, S. G. Flantua, E. L. Dantas, R. Dino, D. A. do Carmo & F. Chemale (2017): The Amazon at sea: onset and stages of the Amazon River from a marine record, with special reference to Neogene plant turnover in the drainage basin. – Global Planet Change, **153**: 51–65.

Jenkins, C. N., S. L. Pimm & L. N. Joppa (2013): Global patterns of terrestrial vertebrate diversity and conservation. – Proceedings of the National Academy of Sciences, **110**: E2602–E2610.

Kahn, T. R., E. La Marca, S. Lötters, J. L. Brown, E. Twomey, & A. Amézquita (2016): Aposematic poison frogs (Dendrobatidae) of the Andean countries: Bolivia, Colombia, Ecuador, Perú and Venezuela. Conservation International Tropical Field Guide Series. – Arlington, Conservation International.

Kimura, M. (1980): A simple method for estimating evolutionary rate of base substitutions through comparative studies of nucleotide sequences. – Journal of Molecular Evolution, **16**: 111–120.

Kumar, S., G. Stecher, M. Li, C. Knyaz, & K. Tamura (2018): MEGA X: molecular evolutionary genetics analysis across computing platforms. – Molecular Biology and Evolution, **35**: 1547.

Landis, M. J., N. J. Matzke, B. R. Moore & J. P. Huelsenbeck (2013): Bayesian analysis of biogeography when the number of areas is large. – Systematic Biology, **62**: 789–804.

Leite, R. N. & D. S. Rogers (2013): Revisiting Amazonian phylogeography: insights into diversification hypotheses and novel perspectives. – Organisms Diversity & Evolution, **13**: 639–664.

Lougheed, S. C., C. Gascon, D. A. Jones, J. P. Bogart & P. T. Boag (1999): Ridges and rivers: a test of competing hypotheses of Amazonian diversification using a dart-poison frog (*Epipedobates femoralis*). – Proceedings of the Royal Society of London, **266**: 1829–1835.

Lötters, S., K.-H. Jungfer, F.-W. Henkel & W. Schmidt (2007): Poison frogs. Biology, species and captive husbandry. – Frankfurt am Main, Chimaira.

Lötters, S., A. van der Meijden, D. Rödder, T. E. Köster, T. Kraus, E. La Marca, C. F. B. Haddad & M. Veith (2010): Reinforcing and expanding the predictions of the disturbance vicariance hypothesis in Amazonian harlequin frogs: a molecular phylogenetic and climate envelope modelling approach. – Biodiversity and Conservation, **19**: 2125–2146.

Lynch, J. D. (1979): The amphibians of the lowland tropical forests. – pp. 189–215 in: Duellman, W. E. (ed.): The South American herpetofauna: its origin, evolution and dispersal. – Lawrence, The University of Kansas.

Manichanh, C., C. E. Chapple, L. Frangeul, K. Gloux, R. Guigo & J. Dore (2008): A comparison of random sequence reads versus 16S rDNA sequences for estimating the biodiversity of a metagenomic library. – Nucleic Acids Research, **36**: 5180–5188.

Marin da Fonte, L. F., M. Mayer & S. Lötters (2019): Long-distance dispersal in amphibians. – Frontiers of Biogeography, **11**: e44577.

Massana, R., J. Castresana, V. alagué, L. Guillou, K. Romari, A. Groisillier, K. Valentin & C. Pedrós-Alió (2004): Phylogenetic and ecological analysis of novel marine stramenopiles. – Applied and Environmental Microbiology, **70**: 3528–3534.

Matzke, N. J. (2013): BioGeoBEARS: Biogeography with Bayesian (and Likelihood) Evolutionary Analysis in R Scripts. – R Package, version 0.2, 2013. Available from: http://R-Forge.R-project.org/projects/splits, accessed 5 May 2022.

Mayer, M., L. F. Marin da Fonte & S. Lötters (2019): Mind the gap! A review of Amazonian anurans in GenBank. – Salamandra, **55**: 89–96.

Minh, B. Q., M. A. T. Nguyen & A. von Haeseler (2013): Ultrafast approximation for phylogenetic bootstrap. – Molecular Biology and Evolution, **30**: 1188–1195.

Montanarin, A., W. del Toro-Orozco & E. E. Ramalho (2017): First record of aggregative behaviour in the territorial poison frog *Ameerega hahneli* (Anura: Dendrobatidae): A strategy for surviving in the Central Amazonian flooded forest? – Salamandra, **53**: 319–320.

Múrias dos Santos, A., M. P. Cabezas, A. I. Tavares, R. Xavier, & M. Branco (2016): TcsBU: a tool to extend TCS network layout and visualization. – Bioinformatics, **32**: 627–628.

Nguyen, L. T., H. A. Schmidt, A. von Haeseler, & B. Q. Minh (2015): IQ-TREE: a fast and effective stochastic algorithm for estimating maximum-likelihood phylogenies. – Molecular Biology and Evolution, **32**: 268–274.

Noonan, B. P. & P. Gaucher (2005): Phylogeography and demography of Guianan harlequin toads (*Atelopus*): diversification within a refuge. – Molecular Ecology, **14**: 3017–3031.

Oliveira, B. F., V. A. São-Pedro, G. Santos-Barrera, C. Penone & G. C. Costa (2017): AmphiBIO, a global database for amphibian ecological traits. – Scientific Data, **4**: 1–7.

Padial, J. M. & I.De la Riva (2009): Integrative taxonomy reveals cryptic Amazonian species of *Pristimantis* (Anura: Strabomantidae). – Zoological Journal of the Linnean Society, **155**: 97–122.

Palumbi, S., A. Martin, S. Romano, W. O. McMillan, L. Stice & G. Grabowski (2002): The simple fool's guide to PCR. – Honolulu, University of Hawaii.

Paradis, E. & K. Schliep (2019): APE 5.0: an environment for modern phylogenetics and evolutionary analyses in R. – Bioinformatics, **35**: 526–528.

Pašukonis, A., M. C. Loretto & B. Rojas (2019): How far do tadpoles travel in the rainforest? Parent-assisted dispersal in poison frogs. – Evolutionary Ecology, **33**: 613–623.

Peloso, P. L., M. J. Sturaro, M. C. Forlani, P. Gaucher, A. P. Motta & W. C. Wheeler (2014): Phylogeny, taxonomic revision and character evolution of the genera *Chiasmocleis* and *Syncope* (Anura, Microhylidae) in Amazonia, with descriptions of three new species. – Bulletin of the American Museum of Natural History, **2014**: 1–112.

Penner, J. & M.-O. Rödel (2019): Keep it simple? Dispersal abilities can explain why species range sizes differ, the case study of West African amphibians. – Acta Oecologia, **94**: 41–46.

Pirani, R. M., P. L. Peloso, J. R. Prado, É. M. Polo, L. L. Knowles, S. R. Ron, M. T. Rodrigues, M. J. Sturaroh & F. P. Werneckai (2020): Diversification history of clown tree frogs in Neotropical rainforests (Anura, Hylidae, *Dendropsophus leucophyllatus* group). – Molecular Phylogenetics and Evolution, **150**: 106877.

Pirani, R. M., F. P. Werneck, A. T. Thomaz, M. L. Kenney, M. J. Sturaro, T. C. Ávila-Pires, P. L. V. Peloso, M. T. Rodrigues & L. L. Knowles (2019): Testing main Amazonian rivers as barriers across time and space within widespread taxa. – Journal of Biogeography, **46**: 2444–2456.

Puillandre, N., S. Brouillet & G. Achaz (2020): ASAP: Assemble species by automatic partitioning. – Molecular Ecology Resources, **21**: 609–620.

Pons, J., T. G. Barraclough, J. Gomez-Zurita, A. Cardoso, D. P. Duran, S. Hazell, S. Kamoun, W. D. Sumlin & A. P. Vogler (2006): Sequence-based species delimitation for the DNA taxonomy of undescribed insects. – Systematic Biology, **55**: 595–609.

Posada, D. & K. A. Crandall (2000): TCS: a computer program to estimate gene genealogies. – Molecular Ecology, **9**: 1657–1660.

Rambaut, A., A. J. Drummond, D. Xie, G. Baele & M. A. Suchard (2018): Posterior summarization in Bayesian phylogenetics using Tracer 1.7. – Systematic Biology, **67**: 901–904.

Ree, R. H. & S. A. Smith (2008): Maximum likelihood inference of geographic range evolution by dispersal, local extinction and cladogenesis. – Systematic Biology, **57**: 4–14.

Réjaud, A., M. T. Rodrigues, A. J. Crawford, S. Castroviejo-Fisher, A. F. Jaramillo, J. C. Chaparro, F. Glaw, G. Gagliardi-Urrutia, J. Moravec, I. J. De la Riva, P. Perez, A. P. Lima, F. P. Werneck, T. Hrbek, S. R. Ron, R.

Ernst, P. J. R. Kok, A. Driskell, J. Chave & A. Fouquet (2020): Historical biogeography identifies a possible role of Miocene wetlands in the diversification of the Amazonian rocket frogs (Aromobatidae: *Allobates*). – Journal of Biogeography, **47**: 2472–2482.

Ribas, C. C., A. Aleixo, A. C. Nogueira, C. Y. Miyaki & J. Cracraft (2012): A palaeobiogeographic model for biotic diversification within Amazonia over the past three million years. – Proceedings of the Royal Society B: Biological Sciences, **279**: 681–689.

Ripley, B., B. Venables, D. M. Bates, K. Hornik, A. Gebhardt, D. Firth & M. B. Ripley (2015): MASS. Available from: https://cran.r-project.org/web/packages/MASS/MASS.pdf, 780, accessed 30 July 2022.

Roberts, J. L., J. L. Brown, R. von May, W. Arizabal, A. Presar, R. Symula & R. Schulte (2006): Phylogenetic relationships among poison frogs of the genus *Dendrobates* (Dendrobatidae): a molecular perspective from increased taxon sampling. – Herpetological Journal, **16**: 377–385.

Rojas, R. R., Fouquet, A., Ron, S. R., Hernández-Ruz, E. J., Melo-Sampaio, P. R., Chaparro, J. C., R. Vogt, V. Tadeu de Carvalho, L. Cardoso, R. Avila, I. Pires, M. Gordo & T. Hrbek (2018): A pan-Amazonian species delimitation: high species diversity within the genus *Amazophrynella* (Anura: Bufonidae). – PeerJ, **6**: e4941.

Ronquist, F. (1997): Dispersal-vicariance analysis: a new approach to the quantification of historical biogeography. – Systematic Biology, **46**: 195–203.

Ronquist, F. & J. P. Huelsenbeck (2003): MrBayes 3: Bayesian phylogenetic inference under mixed models. – Bioinformatics, **19**: 1572–1574.

Rozas, J., A. Ferrer-Mata, J. C. Sánchez-DelBarrio, S. Guirao-Rico, P. Librado, S. E. Ramos-Onsins & A. Sánchez-Gracia (2017): DnaSP 6: DNA Sequence Polymorphism Analysis of Large Datasets. – Molecular Biology and Evolution, **34**: 3299–3302.

Rull, V. & A. C. Carnaval (2020): Neotropical diversification: patterns and processes. – Berlin etc., Springer.

Santos, J. C., L. A. Coloma, K. Summers, J. P. Caldwell, R. Ree & D. C. Cannatella (2009): Amazonian amphibian diversity is primarily derived from Late Miocene Andean lineages. – PLoS Biology, **7**: e1000056.

Schlüter, A. (2005): Amphibien an einem Stillgewässer in Peru. – Frankfurt am Main, Chimaira.

Searcy, C. A., B. Gilbert, M. Krkošek, L. Rowe & S. J. McCauley (2018): Positive correlation between dispersal and body size in green frogs (*Rana clamitans*) naturally colonizing an experimental landscape. – Canadian Journal of Zoology, **96**: 1378–1384.

Shephard, G. E., R. D. Müller, L. Liu & M. Gurnis (2010): Miocene drainage reversal of the Amazon River driven by plate-mantle interaction. – Nature Geoscience, **3**: 870–875.

Silverstone, P. A. (1976): A revision of the poison-arrow frogs of the genus *Phyllobates* Bibron in Sagra (Family Dendrobatidae). – Natural History Museum of Los Angeles County, Science Bulletin, **27**: 1–53.

Spix, J. B. (1824): Animalia Nova sive Species Novae Testudinum et Ranarum quas in Itinere per Brasiliam Annis MDCCCXVII–MDCCCXX Jussu et Auspiciis Maximiliani Josephi I. Bavariae Regis. – München, Hübschmann.

Tagliacollo, V. A., F. F. Roxo, S. M. Duke-Sylvester, C. Oliveira & J. S. Albert (2015): Biogeographical signature of river capture events in Amazonian lowlands. – Journal of Biogeography, **42**: 2349–2362.

Talavera, G. & J. Castresana (2007): Improvement of phylogenies after removing divergent and ambiguously aligned blocks from protein sequence alignments. – Systematic Biology, **56**: 564–577.

Trakimas, G., R. J. Whittaker & M. K. Borregaard (2016): Do biological traits drive geographical patterns in European amphibians? – Global Ecology and Biogeography, **25**: 1228–1238.

Twomey, E., V. Morales & K. Summers (2008): Evaluating condition-specific and asymmetric competition in a species-distribution context. – Oikos, **117**: 1175–1184.

Vacher, J. P., P. J. Kok, M. T. Rodrigues, J. D. Lima, A. Lorenzini, Q. Martinez, M. Fallet, E. A. Courtois, M. Blanc, P. Gaucher, M. Dewynter, R. Jairam, P. Ouboter, C. Thébaud & A. Fouquet (2017): Cryptic diversity in Amazonian frogs: Integrative taxonomy of the genus *Anomaloglossus* (Amphibia: Anura: Aromobatidae) reveals a unique case of diversification within the Guiana Shield. – Molecular Phylogenetics and Evolution, **112**: 158–173.

Vences, M., M. Thomas, R. Bonett & D. Vieites (2005): Deciphering amphibian diversity through DNA barcoding: chances and challenges. – Philosophical Transactions of the Royal Society B, **360**: 1859–1868.

Vences, M., M. Thomas, A. van der Meijden, Y. Chiari & D. R. Vieites (2005b): Comparative performance of the 16S rRNA gene in DNA barcoding of amphibians. – Frontiers in Zoology, **2**: 1–12.

Vences, M. & D. B. Wake (2007): Speciation, species boundaries and phylogeography of amphibians. – pp. 2613–2669 in: Heatwole, H. H. & M. Tyler (eds): Amphibian biology. – Chipping Norton, Surrey Beatty and Sons.

Wollenberg, K. C., D. R. Vieites, F. Glaw & M. Vences (2011): Speciation in little: the role of range and body size in the diversification of Malagasy mantellid frogs. – BMC Evolutionary Biology, **11**: 1–16.

Supplementary data

The following data are available online:

Supplementary Table S1. List of *Ameerega trivittata* samples processed.

Supplementary Table S2. Uncorrected p-distances.

Supplementary Table S3. GMYC results.

Supplementary Figure S1. BI tree.

Supplementary Figure S2. ML tree.

Supplementary Figure S3. Molecular clock BEAST2.